



HAL
open science

Ancient chicken remains reveal the origins of virulence in Marek's disease virus

Steven Fiddaman, Evangelos A Dimopoulos, Ophélie Lebrasseur, Louis Du Plessis, Bram Vrancken, Sophy Charlton, Ashleigh F Haruda, Kristina Tabbada, Patrik G Flammer, Stefan Dascalu, et al.

► **To cite this version:**

Steven Fiddaman, Evangelos A Dimopoulos, Ophélie Lebrasseur, Louis Du Plessis, Bram Vrancken, et al.. Ancient chicken remains reveal the origins of virulence in Marek's disease virus. *Science*, 2023, 382 (6676), pp.1276-1281. 10.1126/science.adg2238 . hal-04782521

HAL Id: hal-04782521

<https://hal.science/hal-04782521v1>

Submitted on 14 Nov 2024

HAL is a multi-disciplinary open access archive for the deposit and dissemination of scientific research documents, whether they are published or not. The documents may come from teaching and research institutions in France or abroad, or from public or private research centers.

L'archive ouverte pluridisciplinaire **HAL**, est destinée au dépôt et à la diffusion de documents scientifiques de niveau recherche, publiés ou non, émanant des établissements d'enseignement et de recherche français ou étrangers, des laboratoires publics ou privés.



Distributed under a Creative Commons Attribution 4.0 International License

1
2 Title: Ancient chicken remains reveal the origins of virulence in Marek's
3 disease virus

4 **Authors:**

5 Steven R Fiddaman^{1†*}, Evangelos A Dimopoulos^{2,3†}, Ophélie Lebrasseur^{4,5}, Louis du Plessis^{6,7}, Bram
6 Vrancken^{8,9}, Sophy Charlton^{2,10}, Ashleigh F Haruda², Kristina Tabbada², Patrik G Flammer¹, Stefan
7 Dascalu¹, Nemanja Marković¹¹, Hannah Li¹², Gabrielle Franklin¹³, Robert Symmons¹⁴, Henriette
8 Baron¹⁵, László Daróczy-Szabó¹⁶, Dilyara N Shaymuratova¹⁷, Igor V Askeyev¹⁷, Olivier Putelat¹⁸,
9 Maria Sana¹⁹, Hossein Davoudi²⁰, Homa Fathi²⁰, Amir Saed Mucheshi²¹, Ali Akbar Vahdati²²,
10 Liangren Zhang²³, Alison Foster²⁴, Naomi Sykes²⁵, Gabrielle Cass Baumberg², Jelena Bulatović²⁶,
11 Arthur O Askeyev¹⁷, Oleg V Askeyev¹⁷, Marjan Mashkour^{20,27}, Oliver G Pybus^{1,28}, Venugopal
12 Nair^{1,29}, Greger Larson^{2‡}, Adrian L Smith^{1*‡}, Laurent AF Frantz^{30,31*‡}

13 **Affiliations:**

14 ¹Department of Biology, University of Oxford, Oxford, UK

15 ²The Palaeogenomics & Bio-Archaeology Research Network, Research Laboratory for Archaeology
16 and History of Art, University of Oxford, Oxford, UK

17 ³Department of Veterinary Medicine, University of Cambridge, Cambridge, UK

18 ⁴Centre d'Anthropobiologie et de Génomique de Toulouse, Toulouse, France

19 ⁵Instituto Nacional de Antropología y Pensamiento Latinoamericano, Ciudad Autónoma de Buenos
20 Aires, Buenos Aires, Argentina

21 ⁶Department of Biosystems Science and Engineering, ETH Zurich, Basel, Switzerland

22 ⁷Swiss Institute of Bioinformatics, Lausanne, Switzerland

23 ⁸Department of Microbiology, Immunology and Transplantation, Rega Institute, KU Leuven, Leuven,
24 Belgium

25 ⁹Spatial Epidemiology Lab (SPELL), Université Libre de Bruxelles, Brussels, Belgium

26 ¹⁰BioArCh, Department of Archaeology, University of York, York, UK

27 ¹¹Institute of Archaeology, Belgrade, Serbia

28 ¹²Institute of Immunity and Transplantation, University College London, London, UK

29 ¹³Silkie Club of Great Britain, Charing, UK

- 30 ¹⁴Fishbourne Roman Palace, Fishbourne, UK
- 31 ¹⁵Leibniz-Zentrum für Archäologie, Mainz, Germany
- 32 ¹⁶Medieval Department, Budapest History Museum, Budapest, Hungary
- 33 ¹⁷Laboratory of Biomonitoring, The Institute of Problems in Ecology and Mineral Wealth, Tatarstan
34 Academy of Sciences, Kazan, Russia
- 35 ¹⁸Archéologie Alsace - PAIR, Bas-Rhin, France
- 36 ¹⁹Departament de Prehistòria, Universitat Autònoma de Barcelona, Barcelona, Spain
- 37 ²⁰Bioarchaeology Laboratory, Central Laboratory, University of Tehran, Tehran, Iran
- 38 ²¹Department of Art and Architecture, Payame Noor University (PNU), Tehran, Iran
- 39 ²²Provincial Office of the Iranian Center for Cultural Heritage, Handicrafts and Tourism Organisation,
40 Bojnord, Iran
- 41 ²³Department of Archaeology, School of History, Nanjing University, China
- 42 ²⁴Headland Archaeology, Edinburgh, UK
- 43 ²⁵Department of Archaeology, University of Exeter, Exeter, UK
- 44 ²⁶Department of Historical Studies, University of Gothenburg, Gothenburg, Sweden
- 45 ²⁷CNRS, National Museum Natural History Paris, Paris, France
- 46 ²⁸Department of Pathobiology and Population Sciences, Royal Veterinary College, London, UK
- 47 ²⁹Viral Oncogenesis Group, Pirbright Institute, Woking, UK
- 48 ³⁰Department of Veterinary Sciences, Ludwig Maximilian University of Munich, Munich, Germany
- 49 ³¹School of Biological and Chemical Sciences, Queen Mary University of London, London, UK
- 50 †joint-first author
- 51 ‡ co-senior authors
- 52 * corresponding authors. Emails: steven.fiddaman@biology.ox.ac.uk; adrian.smith@biology.ox.ac.uk;
53 laurent.frantz@lmu.de

54 **Abstract:**

55 The dramatic growth in livestock populations since the 1950s has altered the epidemiological and
56 evolutionary trajectory of their associated pathogens. For example, Marek's disease virus (MDV),
57 which causes lymphoid tumors in chickens, has experienced a marked increase in virulence over the
58 last century. Today, MDV infections kill >90% of unvaccinated birds and controlling it costs
59 >US\$1bn annually. By sequencing MDV genomes derived from archeological chickens, we
60 demonstrate that it has been circulating for at least 1000 years. We functionally tested the *Meq*
61 oncogene, one of 49 viral genes positively selected in modern strains, demonstrating that ancient
62 MDV was likely incapable of driving tumor formation. Our results demonstrate the power of ancient
63 DNA approaches to trace the molecular basis of virulence in economically relevant pathogens.

64
65 **One sentence summary:**

66 Functional paleogenomics reveals the molecular basis for increased virulence in Marek's Disease
67 Virus.

68
69 **Main Text:**

70 Marek's Disease Virus (MDV) is a highly contagious alphaherpesvirus that causes a tumor-associated
71 disease in poultry. At the time of its initial description in 1907, Marek's Disease (MD) was a
72 relatively mild disease with low mortality, characterized by nerve pathology mainly affecting older
73 individuals(1). However, over the course of the 20th century, MDV-related mortality has risen to
74 >90% in unvaccinated chickens. To prevent this high mortality rate, the poultry industry spends more
75 than US\$1 billion per year on health intervention measures, including vaccination(2).

76
77 The increase in virulence and clinical pathology of MDV infection has likely been driven by a
78 combination of factors. Firstly, the growth in the global chicken population since the 1950s led to
79 more viral replication, which increased the supply of novel mutations in the population. In addition,
80 the use of imperfect (also known as 'leaky') vaccines that prevent symptomatic disease but do not
81 prevent transmission of the virus likely shifted selective pressures and led to an accelerated rate of
82 MDV virulence evolution(3). Combined, these factors have altered the evolutionary trajectory,
83 resulting in modern hyper-pathogenic strains. To date, the earliest sequenced MDV genomes were
84 sampled in the 1960s(4), several decades after the first reports of MDV causing tumors(5). As a
85 result, the genetic changes that contributed to the increase in virulence of MDV infection prior to the
86 1960s remain unknown.

87
88 **Marek's disease virus has been circulating in Europe for at least 1000 years**

89 To empirically track the evolutionary change in MDV virulence through time, we generated MDV
90 genome sequences (serotype 1) isolated from the skeletal remains of archeological chickens. We first
91 shotgun sequenced 995 archeological chicken samples excavated from >140 Western Eurasian
92 archeological sites and screened for MDV reads using HAYSTAC(6) with a herpesvirus-specific
93 database. Samples with any evidence of MDV reads were then enriched for viral DNA using a
94 hybridisation-based capture approach based on RNA baits designed to tile the entire MDV genome
95 (excluding one copy of each of the terminal repeats and regions of low complexity). To validate the

96 approach, we also captured and sequenced DNA from the feather of a modern Silkie chicken that
97 presented MDV symptoms. As a negative control, we also included an ancient sample that displayed
98 no evidence of MDV reads following screening (OL1214; Serbia, C14th-15th).

99

100 Using the capture protocol we identified 15 ancient chickens with MDV-specific reads of ≥ 25 bp in
101 length. This approach also yielded a $\sim 4\times$ genome from a modern positive control. We found that the
102 majority of uniquely mapped reads (i.e. 88-99%) generated from ancient samples classified as MDV-
103 positive were ≥ 25 bp, while the majority (i.e. 53-100%) of uniquely mapped reads generated from
104 samples considered MDV-negative were shorter than 25bp. In addition, samples considered MDV-
105 positive yielded between 308 and 133,885 uniquely mapped reads (≥ 25 bp) while samples considered
106 MDV-negative (including a negative control; Table S2) yielded between 0 and 211 uniquely mapped
107 reads of ≥ 25 bp. MDV-positive ancient samples ranged in depth of coverage from $0.13\times$ to $41.92\times$
108 (OL1385; Fig. 1a, Table S2), with seven genomes at $\geq 2\times$ coverage.

109

110 In all positive samples, the proportion of duplicated reads approached 100%, indicating that virtually
111 all of the unique molecules in each library were sequenced at least once (Fig. S1). Reads obtained
112 from MDV-positive ancient samples were characterized by chemical signatures of DNA damage
113 typically associated with ancient DNA (Fig. S2). In contrast, reads obtained from our modern positive
114 control did not show any evidence of DNA damage (Fig. S2). The earliest unequivocally MDV-
115 positive sample (with 4,760 post-capture reads ≥ 25 bp) was derived from a 10th-12th century chicken
116 from Eastern France (Andlau in Fig. 1a; Table S2). Together, these results demonstrate that MDV
117 strains have been circulating in Western Eurasian poultry for at least 1,000 years.

118

119 **Ancient MDV strains are basal to modern lineages**

120 To investigate the relationship between ancient and modern MDV strains, we built phylogenetic trees
121 based on both neighbor-joining (NJ) and maximum likelihood (ML) methods. We first built trees
122 using 10 ancient genomes with at least 1% coverage at a depth of $\geq 5\times$, a modern positive control
123 derived from the present study (OL1099), and 42 modern genomes from public sources (Table S3).
124 Both NJ (Fig. 1b, Fig. S3) and ML trees (Fig. S4) match the previously described general topology(7),
125 in which Eurasian and North American lineages were evident, along with a well-supported (bootstrap:
126 94) ancient clade (Fig 1b). The same topology was also obtained when restricting our ML analysis to
127 include only transversion sites (Fig. S5). Lastly, we built a tree using an outgroup (Meleagrid
128 herpesvirus 1, accession: NC_002641.1) to root our topology (Fig. S6). We obtained a well-supported
129 topology showing that the ancient MDV sequences form a highly supported clade lying basal to all
130 modern MDV strains (including the modern positive control OL1099).

131

132 Next, we built a time-calibrated phylogeny using BEAST (v. 1.10;(8)) that included 31 modern
133 genomes collected since 1968 (Table S3), and four ancient samples with an average depth of coverage
134 $>5\times$ (OL1986, Castillo de Montsoriu, Spain, 1593 cal. CE; OL1385, Buda Castle, Hungary, 1802 cal.
135 CE; OL1389, an additional Buda Castle sample from the same archeological context as OL1385;

136 OL2272, Naderi Tepe, Iran, 1820 cal. CE; Table S1-S2, Fig. 1a). All of the ancient samples were
137 phylogenetically basal to all modern MDV strains. The time of the most recent common ancestor
138 (TMRCA) of the phylogeny was 1602 CE (95% HPD interval 1486 - 1767; Fig. 1c, Table S4).

139
140 As previously reported(7) we found that, aside from a few exceptions, most Eurasian and North
141 American MDV strains formed distinct clades (Fig. 1b), suggesting that there has been little recent
142 transatlantic exchange of the virus. The inclusion of time-stamped ancient MDV sequences improved
143 the accuracy of the molecular clock analysis, and pushed back the TMRCA of all modern MDV
144 sequences, from 1922-1952(7) to 1881 (95% HPD interval 1822 - 1929; Table S4). Our mean
145 TMRCA of modern MDV is concordant with a recent estimate that incorporated 26 modern MDV
146 genomes from East Asian chickens (1880, 95% HPD 1772-1968;(9)). This phylogenetic analysis
147 implies that the two major modern clades of MDV were likely established before the earliest
148 documented increases in MDV virulence in the 1920s. Furthermore, since birds infected with highly
149 virulent MDV would not have survived a transatlantic crossing, a TMRCA of 1938 (95% HPD 1914 -
150 1958) for the clade containing the earliest North American sample (CU2, 1968; accession:
151 EU499381.1) could be consistent with the virus having been transmitted prior to the most significant
152 virulence increases leading up to the 1960s. These results are also consistent with the hypothesis that
153 Eurasian and North American MDV lineages independently evolved towards increased virulence(7).

154

155 **Virulence factors are among positively selected genes in the modern MDV lineage**

156 The rapid increase in MDV virulence could potentially have been driven by gene loss or gain which
157 would have substantially altered the biology of the virus(10, 11). Analysis of a Hungarian, high
158 coverage, MDV genome (OL1385; >41x) from the 18th - 19th century indicated that it possessed the
159 full complement of genes present in modern sequences. This indicates that there was no gene gain or
160 loss in either ancient or modern lineage (Fig. 2). We also found that all MDV miRNAs, some of
161 which are implicated in pathogenesis and oncogenesis in modern strains(12), were intact and highly
162 conserved in ancient strains (Table S5). Together, these results indicate that the acquisition of
163 virulence most likely resulted not from changes in MDV genome content or organization, but from
164 point mutations.

165

166 In fact, considering sites at which we had coverage for at least two ancient genomes, we identified
167 158 fixed single nucleotide polymorphism (SNPs) between the ancient and modern samples, of which
168 31 were found in intergenic regions and may be candidates for future study of MDV regulatory
169 regions (Table S6). To assess the impact of positive selection on point mutations we performed a
170 branch-site analysis in PAML(13) (ancient sequences as background lineage, modern sequences as
171 foreground lineage) on open reading frames (ORFs) using four ancient MDV genomes (OL1385,
172 OL1389, OL1986 and OL2272). After controlling the false discovery rate using the Benjamini-
173 Hochberg procedure(14), this analysis identified 49 ORFs with significant evidence for positive
174 selection (Fig. 2; Table S7).

175

176 Several positively selected loci identified in this analysis have previously been associated with MDV
177 virulence in modern strains. Some of these are known immune modulators or potential targets of a
178 protective response. This includes ICP4, a large transcriptional regulatory protein involved in innate
179 immune interference. Interestingly, ICP4 appears to be an important target of T cell-mediated
180 immunity against MDV in chickens possessing the B21 Major Histocompatibility Complex (MHC)
181 haplotype(15), and it is plausible that sequence variation in important ICP4 epitopes could confer
182 differential susceptibility to infection.

183
184 We also identified signatures of positive selection in several genes encoding viral glycoproteins (gC,
185 gE, gI, gK and gL). Glycoproteins are important targets for the immune response to MDV(16). In
186 fact, the majority of MDV peptides presented on chicken MHC class II are derived from just four
187 proteins(17), of which two were glycoproteins found to be under selection in our analysis (gE and gI).
188 This result indicates that glycoproteins are likely under selection in MDV because they are immune
189 targets. The limited scope of immunologically important MDV peptides presented by MHC class II
190 may have important implications for vaccine development.

191
192 Positive selection was also detected in the viral chemokine termed viral interleukin-8 (considered a
193 functional ortholog of chicken CXC ligand 13;(18)). Viral IL-8 is an important virulence factor that
194 recruits B cells for lytic replication and CD4+ CD25+ T cells that are transformed to generate
195 lymphoid tumors. Viruses that lack vIL-8 are severely impaired in the establishment of infection and
196 generation of tumors through bird-to-bird transmission(19), so sequence variation in this gene could
197 plausibly impact transmission.

198
199 **The key oncogene of MDV has experienced positive selection and an ordered loss of tetraproline**
200 **motifs**

201 Our selection scan also identified *Meq*, a transcription factor considered to be the master regulator of
202 tumor formation in MDV(20). In fact, the *Meq* coding sequence had the greatest average pairwise
203 divergence between ancient and modern strains across the entirety of the MDV genome (Fig. 2),
204 implying there were numerous sequence changes along the branch leading to modern samples.
205 Animal experiments have demonstrated that *Meq* is essential for tumor formation(20) and
206 polymorphisms in this gene, even in the absence of variants elsewhere in the genome, are known to
207 confer significant differences in strain virulence or vaccine breakthrough ability(21).

208
209 *Meq* exerts transcriptional control on downstream gene targets (both in the host and viral genome) via
210 its C-terminal transactivation domain. This domain is characterized by PPPP (tetraproline) repeats
211 spaced throughout the second half of the protein, and the number of tetraproline repeats is inversely
212 proportional to the virulence of the MDV strain(22). The difference in the number of tetraproline
213 repeats in most strains is the result of point mutations rather than deletion or duplication; these strains
214 are considered ‘standard length’-*Meq* (339 amino acids). In some strains, however, tetraproline
215 repeats have been duplicated (‘long’-*Meq* strains, 399 amino acids) or deleted (‘short’-*Meq* strains,

216 298 amino acids, or ‘very short’-Meq, 247 amino acids). These mutations have led to varying
217 numbers of tetraproline repeats between strains.

218

219 We did not find any evidence of duplication or deletion in ancient Meq sequences, indicating that
220 there are ‘standard length’-Meq. We then identified point mutations in a database containing four
221 ancient Meq sequences (OL1385, OL1389, OL1986 and OL2272) along with 408 modern ‘standard
222 length’-Meq sequences (Table S8). This analysis demonstrated that ancient Meq possessed six intact
223 tetraproline motifs while all modern ‘standard length’-Meq sequences had between two and five. All
224 ancient Meq sequences had a unique additional intact tetraproline motif at amino acids 290-293. This
225 tetraproline motif was disrupted by a point mutation – causing a Proline to Histidine change – in the
226 recent evolutionary history of ‘standard length’-Meq MDV strains.

227

228 To further explore the virulence-related disruption of tetraprolines in modern *Meq* sequences, we
229 constructed a phylogeny of *Meq* sequences (Fig. 3a). Mapping the tetraproline content of each
230 sequence on the phylogeny indicated that tetraprolines have been lost in a specific order. Following
231 the universal disruption of the 6th tetraproline through a point mutation (at amino acids 290-293) at the
232 base of the modern MDV lineage, the 4th tetraproline was disrupted at the base of two major lineages
233 (amino acids 216-219). Disruption of the 4th tetraproline was followed in seven independent lineages
234 by the disruption of the 2nd tetraproline (amino acids 175-178), and then by the loss of either the 1st
235 (amino acids 152-155) or the 5th tetraproline (amino acids 232-235) in six lineages (Fig. 3a-b).

236

237 Interestingly, our analysis indicated that the 2nd and 4th tetraprolines (codons 176 and 217) were under
238 positive selection (Table S7). Although there were some observations of virus lineages exhibiting an
239 alternative loss order (e.g. the occasional loss of the 3rd tetraproline (amino acids 191-194) following
240 the loss of the 4th), such lineages are not widespread, suggesting that they may become stuck in local
241 fitness peaks and are outcompeted by lineages following the order described above. The independent
242 recapitulation of this pattern in different lineages suggests loss of tetraproline motifs acts as a ratchet,
243 whereby each subsequent loss results in an increase in virulence, and once lost, motifs are unlikely to
244 be regained.

245

246 **Ancient Meq is a weak transactivator that likely did not drive tumor formation**

247 The initial description of MD in 1907 did not mention tumors(1). Given the degree of sequence
248 differentiation observed between ancient and modern *Meq* genes, it is possible that ancient MDV
249 genotypes were incapable of driving lymphoid cell transformation. To test this hypothesis
250 experimentally, we assessed whether ancient Meq possessed lower transactivation capabilities,
251 compared to modern strains, in a cultured cell-based assay.

252

253 To do so, we synthesized an ancient *Meq* gene based on our highest coverage ancient sample
254 (OL1385; Buda Castle, Hungary; 1802 cal. CE) and experimentally tested its transactivation function.
255 We also cloned ‘very virulent’ modern pathotype strains (RB1B and Md5), which each differ from
256 ancient Meq at 13-14 amino acid positions (Fig. 3c; Table S9). All the Meq proteins were expressed

257 in cells alongside a chicken protein (c-Jun), with which Meq forms a heterodimer, and a luciferase
258 reporter containing the Meq binding (AP-1) sequence.

259

260 Relative to the baseline signal, the transactivation of the ‘very virulent’ Meq strains RB1B and Md5
261 were 7.5 and 10 times greater, respectively (Fig. 3d). Consistent with previous reports(23), removal of
262 the partner protein, c-Jun, from RB1B resulted in severe abrogation of the transactivation capability
263 (Fig. 3d). Ancient Meq exhibited a ~2.5-fold increase in transactivation relative to the baseline, but
264 was substantially lower (3-4-fold) than Meq from the two ‘very virulent’ pathotypes (Fig. 3d). The
265 ancient Meq was thus a demonstrably weaker transactivator than Meq from modern strains of MDV.

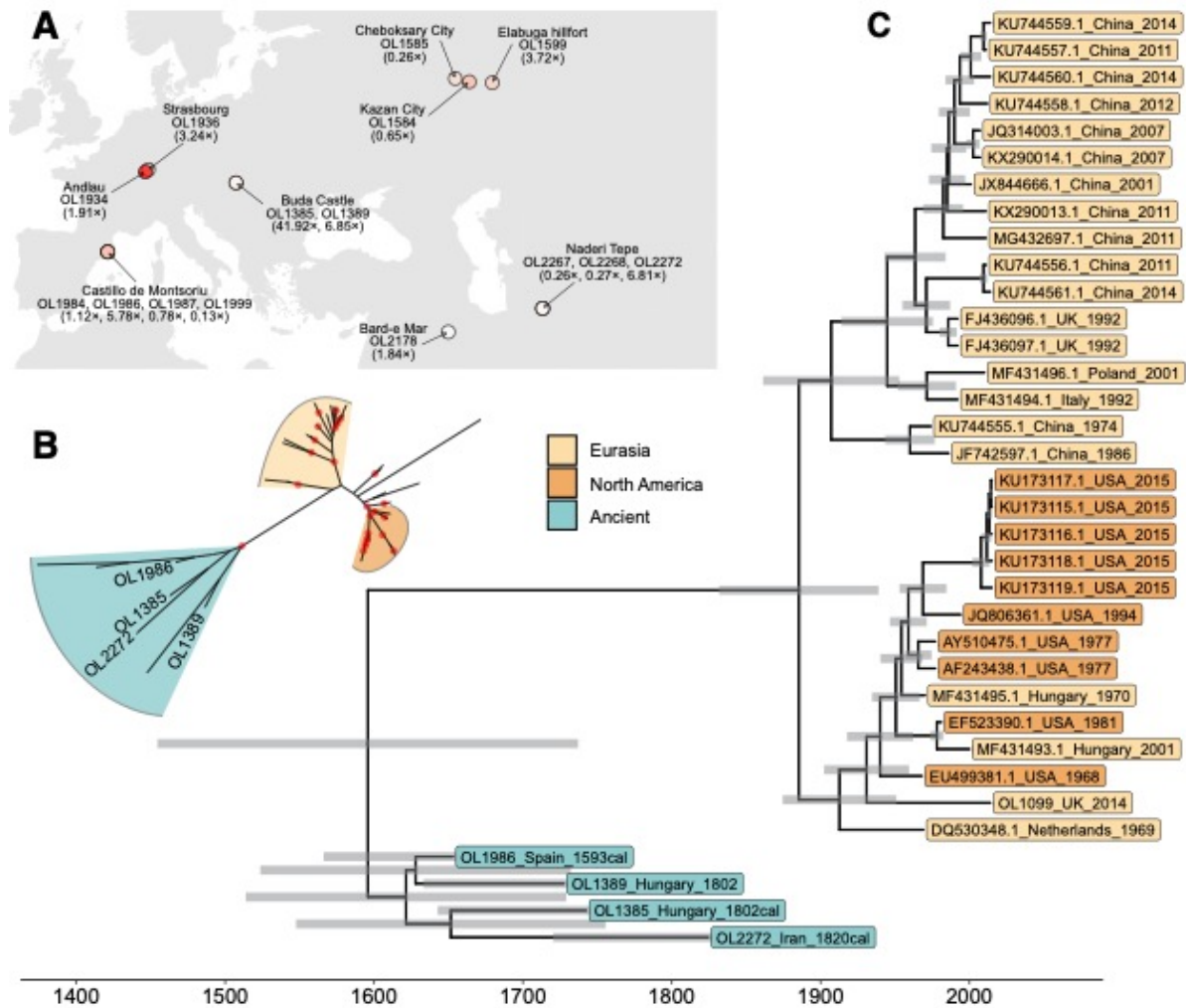
266

267 Given that the transcriptional regulation of target genes (both host and virus) by *Meq* is directly
268 related to oncogenicity(20, 23), it is likely that the weaker transactivation we demonstrate is
269 associated with reduced or absent tumor formation. These data indicate that ancient MDV strains
270 were unlikely to cause tumors, and were less pathogenic than modern strains. Ancient MDV likely
271 established a chronic infection characterized by slower viral replication, low levels of viral shedding
272 and low clinical pathology, which acted to facilitate maximal lifetime viral transmission in pre-
273 industrialized, low-density settings.

274

275 **Conclusion**

276 Overall, our results demonstrate that Marek’s Disease Virus has been circulating in Western Eurasia
277 for at least the last millennium. By reconstructing and functionally assessing ancient and modern
278 genomes, we showed that ancient MDV strains were likely substantially less virulent than modern
279 strains, and that the increase in virulence took place over the last century. Along with changes in
280 several known virulence factors, we identified sequence changes in the *Meq* gene – the master
281 regulator of oncogenesis – that drove its enhanced ability to transactivate its target genes and drive
282 tumor formation. The historical perspective that our results provide can form the basis on which to
283 rationally improve modern vaccines, and track or even predict future virulence changes. Lastly, our
284 results highlight the utility of functional paleogenomics to generate insights into the evolution and
285 fundamental biological workings of pathogen virulence.



287

288

289

290

291

292

293

294

295

296

297

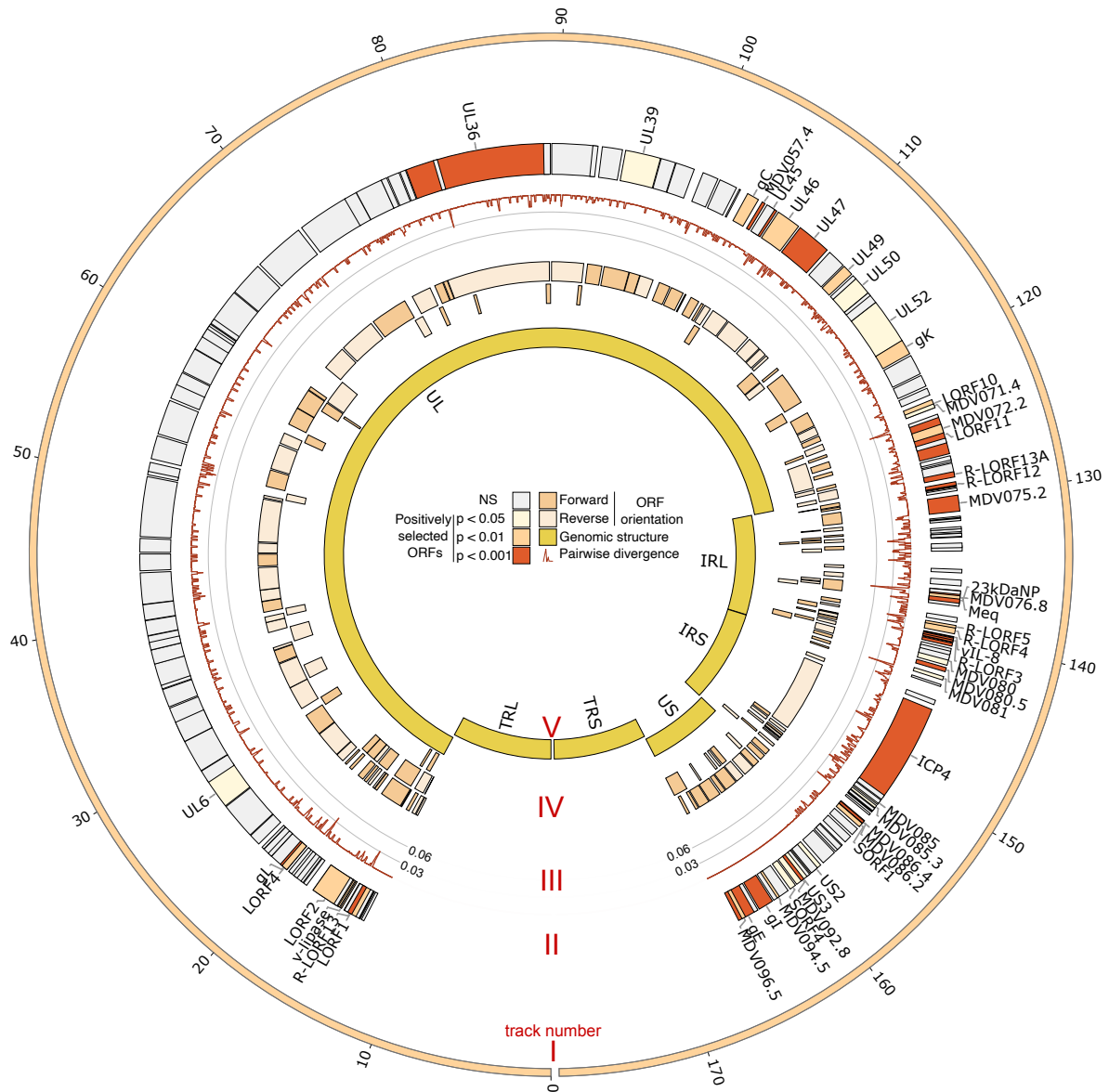
298

299

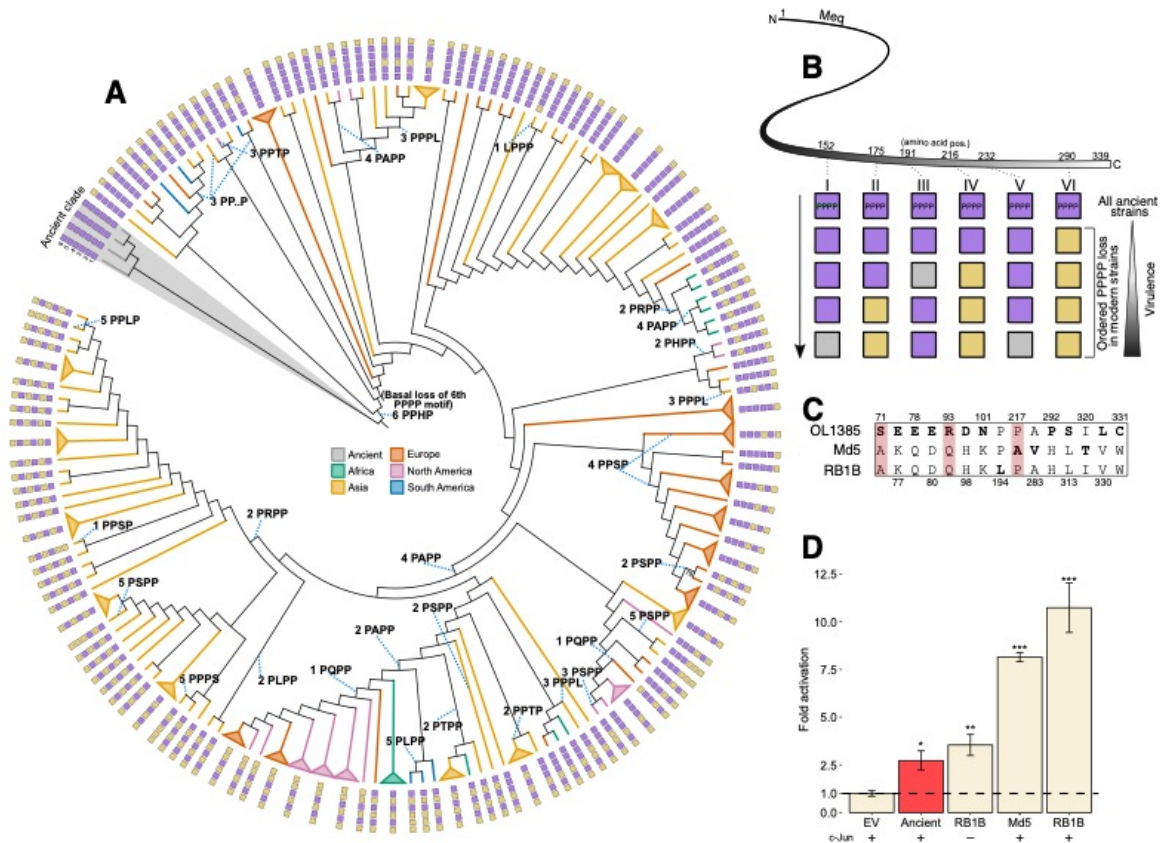
300

301

Fig. 1. Locations of MDV-positive samples and time-scaled phylogeny. (A) Map showing the locations of screened archeological chicken samples that were positive for MDV sequence. Colored circles indicate sample dates (either from calibrated radiocarbon dating or estimated from archeological context; Table S1). Average sequencing depth following capture is given in parentheses under sample names. If more than one sample was derived from the same site, this is indicated by a list of sample identifiers (beginning ‘OL’) and sequencing depths in parentheses. (B) Unrooted neighbor-joining tree of 42 modern and 10 ancient genomes. Only the four high-coverage ancient samples used in our BEAST analysis were labeled in this tree (Table S2). Nodes with bootstrap support of >90 are indicated by red dots. (C) Time-scaled maximum clade credibility tree of ancient and modern MDV sequences using the uncorrelated lognormal relaxed clock model (UCLD) and the general time-reversible (GTR) substitution model. Gray bars indicate the 95% highest posterior density (HPD) for the age of each node. The ‘cal’ suffix for ancient samples indicates that samples were radiocarbon dated and these date distributions were used as priors for the molecular clock analyses(24).



302
 303 **Fig. 2. Branch-site selection analysis of MDV genomes.** The MDV genome is represented as a
 304 circular structure with gross genomic architecture displayed on the innermost track (track V) and
 305 genomic coordinates shown on the outermost track (units: $\times 10^3$ kb; track I). Since the long terminal
 306 repeat (TRL) and short terminal repeat (TRS) are copies of the long internal repeat (IRL) and the
 307 short internal repeat (IRS), respectively, selection analysis excluded the TRL and the TRS regions,
 308 leaving only the unique long (UL) and unique short (US) regions along with the two internal repeats.
 309 Results of the positive selection analysis are displayed on track II, where open reading frames (ORFs)
 310 are shaded according to the strength of statistical support (corrected P-values) for positive selection.
 311 Sliding window average pairwise divergence between ancient and modern samples is shown on track
 312 III, and ORF orientation is shown on track IV.



313
 314 **Fig. 3. *Meq* has undergone ordered loss of tetraproline repeats and increased transactivation**
 315 **ability.** (A) Phylogenetic analysis of 412 *Meq* sequences of standard length (1017 bp). The outermost
 316 track shows the integrity of each tetraproline motif (purple squares = intact; yellow squares =
 317 disrupted). The mutations that disrupt the tetraproline motif are linked by dotted blue lines (e.g. ‘4
 318 PAPP’ indicates that the 4th tetraproline motif is disrupted by a proline-to-alanine substitution in the
 319 second proline position. ‘3 PP..P’ denotes a deletion of the 3rd proline in the 3rd tetraproline motif). For
 320 a complete version of this figure, see Fig. S7. (B) Proposed model for the most common ordered loss
 321 of tetraproline motifs in *Meq*. Purple and green boxes indicate presence and absence of an intact
 322 tetraproline, respectively. The gray box on the third row indicates that the 3rd tetraproline is
 323 occasionally lost after the 6th, but typically only in terminal branches. The two gray boxes in the
 324 bottom row indicate that it is either the 1st or 5th tetraproline that is lost at this point. (C) Positions of
 325 amino acid differences between the ancient Hungarian MDV strain (OL1385) and the two modern
 326 strains (RB1B and Md5). Positions that were also found to be under positive selection are highlighted
 327 in red. (D) The transactivation ability of *Meq* reconstructed from an ancient Hungarian MDV strain
 328 (OL1385) was compared to the transactivation abilities of modern strains: RB1B and Md5 (‘very
 329 virulent’ pathotype). To show the effect of the partner protein c-Jun on transactivation ability, the
 330 strongest transactivator RB1B was tested with (+) and without (-) c-Jun. Transactivation ability is
 331 expressed as fold activation relative to baseline signal from an empty vector (EV). Error bars are
 332 standard deviation, and statistical significance was determined using Dunnett’s test for comparing
 333 several treatment groups with a control. *, P < 0.05; **, P < 0.01; ***, P < 0.001.

334 **References**

- 335 1. J. Marek, Multiple Nervenentzündung (Polyneuritis) bei Hühnern. *Dtsch. Tierarztl. Wochenschr.*
336 **15**, 417–421 (1907).
- 337 2. C. Morrow, F. Fehler, "5 - Marek's disease: A worldwide problem" in *Marek's Disease*, F.
338 Davison, V. Nair, Eds. (Academic Press, Oxford, 2004), pp. 49–61.
- 339 3. A. F. Read, S. J. Baigent, C. Powers, L. B. Kgosana, L. Blackwell, L. P. Smith, D. A. Kennedy,
340 S. W. Walkden-Brown, V. K. Nair, Imperfect Vaccination Can Enhance the Transmission of
341 Highly Virulent Pathogens. *PLoS Biol.* **13**, e1002198 (2015).
- 342 4. C. S. Eidson, K. W. Washburn, S. C. Schmittle, Studies on acute Marek's disease. 9. Resistance
343 to MD by inoculation with the GA isolate. *Poult. Sci.* **47**, 1646–1648 (1968).
- 344 5. N. Osterrieder, J. P. Kamil, D. Schumacher, B. K. Tischer, S. Trapp, Marek's disease virus: from
345 miasma to model. *Nat. Rev. Microbiol.* **4**, 283–294 (2006).
- 346 6. E. A. Dimopoulos, A. Carmagnini, I. M. Velsko, C. Warinner, G. Larson, L. A. F. Frantz, E. K.
347 Irving-Pease, HAYSTAC: A Bayesian framework for robust and rapid species identification in
348 high-throughput sequencing data. *PLoS Comput. Biol.* **18**, e1010493 (2022).
- 349 7. J. Trimpert, N. Groenke, M. Jenckel, S. He, D. Kunec, M. L. Szpara, S. J. Spatz, N. Osterrieder,
350 D. P. McMahon, A phylogenomic analysis of Marek's disease virus reveals independent paths to
351 virulence in Eurasia and North America. *Evol. Appl.* **10**, 1091–1101 (2017).
- 352 8. A. J. Drummond, M. A. Suchard, D. Xie, A. Rambaut, Bayesian phylogenetics with BEAUti and
353 the BEAST 1.7. *Mol. Biol. Evol.* **29**, 1969–1973 (2012).
- 354 9. K. Li, Z. Yu, X. Lan, Y. Wang, X. Qi, H. Cui, L. Gao, X. Wang, Y. Zhang, Y. Gao, C. Liu,
355 Complete genome analysis reveals evolutionary history and temporal dynamics of Marek's
356 disease virus. *Front. Microbiol.* **13**, 1046832 (2022).
- 357 10. K. Majander, S. Pfrengle, A. Kocher, J. Neukamm, L. du Plessis, M. Pla-Díaz, N. Arora, G.
358 Akgül, K. Salo, R. Schats, S. Inskip, M. Oinonen, H. Valk, M. Malve, A. Kriiska, P. Onkamo, F.
359 González-Candelas, D. Kühnert, J. Krause, V. J. Schuenemann, Ancient Bacterial Genomes
360 Reveal a High Diversity of *Treponema pallidum* Strains in Early Modern Europe. *Curr. Biol.* **30**,
361 3788–3803.e10 (2020).
- 362 11. B. Mühlemann, L. Vinner, A. Margaryan, H. Wilhelmson, C. de la Fuente Castro, M. E.
363 Allentoft, P. de Barros Damgaard, A. J. Hansen, S. Holtsmark Nielsen, L. M. Strand, J. Bill, A.
364 Buzhilova, T. Pushkina, C. Falys, V. Khartanovich, V. Moiseyev, M. L. S. Jørkov, P. Østergaard
365 Sørensen, Y. Magnusson, I. Gustin, H. Schroeder, G. Sutter, G. L. Smith, C. Drostén, R. A. M.
366 Fouchier, D. J. Smith, E. Willerslev, T. C. Jones, M. Sikora, Diverse variola virus (smallpox)
367 strains were widespread in northern Europe in the Viking Age. *Science.* **369** (2020),
368 doi:10.1126/science.aaw8977.
- 369 12. M. Teng, Z.-H. Yu, A.-J. Sun, Y.-J. Min, J.-Q. Chi, P. Zhao, J.-W. Su, Z.-Z. Cui, G.-P. Zhang, J.
370 Luo, The significance of the individual Meq-clustered miRNAs of Marek's disease virus in
371 oncogenesis. *J. Gen. Virol.* **96**, 637–649 (2015).
- 372 13. Z. Yang, PAML 4: phylogenetic analysis by maximum likelihood. *Mol. Biol. Evol.* **24**, 1586–
373 1591 (2007).
- 374 14. Y. Benjamini, Y. Hochberg, Controlling the false discovery rate: A practical and powerful
375 approach to multiple testing. *J. R. Stat. Soc.* **57**, 289–300 (1995).

- 376 15. A. R. Omar, K. A. Schat, Syngeneic Marek's disease virus (MDV)-specific cell-mediated
377 immune responses against immediate early, late, and unique MDV proteins. *Virology*. **222**, 87–
378 99 (1996).
- 379 16. C. J. Markowski-Grimrud, K. A. Schat, Cytotoxic T lymphocyte responses to Marek's disease
380 herpesvirus-encoded glycoproteins. *Vet. Immunol. Immunopathol.* **90**, 133–144 (2002).
- 381 17. S. Halabi, M. Ghosh, S. Stevanović, H.-G. Rammensee, L. D. Bertzbach, B. B. Kaufer, M. C.
382 Moncrieffe, B. Kaspers, S. Härtle, J. Kaufman, The dominantly expressed class II molecule from
383 a resistant MHC haplotype presents only a few Marek's disease virus peptides by using an
384 unprecedented binding motif. *PLoS Biol.* **19**, e3001057 (2021).
- 385 18. S. Haertle, I. Alzuheir, F. Busalt, V. Waters, P. Kaiser, B. B. Kaufer, Identification of the
386 Receptor and Cellular Ortholog of the Marek's Disease Virus (MDV) CXC Chemokine. *Front.*
387 *Microbiol.* **8**, 2543 (2017).
- 388 19. A. T. Engel, R. K. Selvaraj, J. P. Kamil, N. Osterrieder, B. B. Kaufer, Marek's disease viral
389 interleukin-8 promotes lymphoma formation through targeted recruitment of B cells and CD4+
390 CD25+ T cells. *J. Virol.* **86**, 8536–8545 (2012).
- 391 20. B. Lupiani, L. F. Lee, X. Cui, I. Gimeno, A. Anderson, R. W. Morgan, R. F. Silva, R. L. Witter,
392 H.-J. Kung, S. M. Reddy, Marek's disease virus-encoded Meq gene is involved in transformation
393 of lymphocytes but is dispensable for replication. *Proc. Natl. Acad. Sci. U. S. A.* **101**, 11815–
394 11820 (2004).
- 395 21. A. M. Conradie, L. D. Bertzbach, J. Trimpert, J. N. Patria, S. Murata, M. S. Parcels, B. B.
396 Kaufer, Distinct polymorphisms in a single herpesvirus gene are capable of enhancing virulence
397 and mediating vaccinal resistance. *PLoS Pathog.* **16**, e1009104 (2020).
- 398 22. K. G. Renz, J. Cooke, N. Clarke, B. F. Cheetham, Z. Hussain, A. F. M. Fakhrol Islam, G. A.
399 Tannock, S. W. Walkden-Brown, Pathotyping of Australian isolates of Marek's disease virus and
400 association of pathogenicity with meq gene polymorphism. *Avian Pathol.* **41**, 161–176 (2012).
- 401 23. Z. Qian, P. Brunovskis, F. Rauscher 3rd, L. Lee, H. J. Kung, Transactivation activity of Meq, a
402 Marek's disease herpesvirus bZIP protein persistently expressed in latently infected transformed
403 T cells. *J. Virol.* **69**, 4037–4044 (1995).
- 404 24. See Supplementary Information.
- 405 25. Zenodo repository (<https://zenodo.org/records/10022436>; DOI:
406 <https://zenodo.org/doi/10.5281/zenodo.10022428>)
- 407 26. O. Putelat, "Archéozoologie" in *Strasbourg, Bas-Rhin. Rue de Lucerne – Rue du Jeu-de-Paume.*
408 *Rapport de fouille préventive. Volume 1. Le système défensif primitif et le processus*
409 *d'urbanisation d'un secteur du faubourg de la Krutenau du Moyen Âge à nos jours. Rapport de*
410 *fouille préventive, Sélestat : Pôle d'Archéologie Interdépartemental Rhénan, M. Werlé, Ed.*
411 (2015), pp. 98–174.
- 412 27. A. Cicović, D. Radičević, "Arheološka istraživanja srednjovekovnih nalazišta na Rudniku 2009–
413 2013. godine" in *Rudnik 1, istraživanja srednjovekovnih nalazišta (2009-2013. godina), Gornji*
414 *Milanovac, D. Radičević, A. Cicović, Eds. (2013), pp. 19–57.*
- 415 28. N. Marković, J. Bulatović, "Rudnik 2009–2013: rezultati arheozoološke analize" in *Rudnik 1,*
416 *istraživanja srednjovekovnih nalazišta (2009-2013. godina), Gornji Milanovac, A. Cicović, D.*
417 *Radičević, Eds. (2019), pp. 119–129.*
- 418 29. H. Baron, Quasi Liber Et Pictura. Die Tierknochenfunde aus dem Gräberfeld an der Wiener

- 419 Csokorgasse – eine anthrozoologische Studie zu den awarischen Bestattungssitten.
420 *Monographien des RGZM.* **143** (2018).
- 421 30. O. Putelat, thesis, Université de Paris 1 Panthéon-Sorbonne (2015).
- 422 31. M. Popović, *Manastir Studenica – arheološka otkrića* (Republički zavod za zaštitu spomenika
423 kulture, Arheološki institut, Beograd, 2015).
- 424 32. N. Marković, "Ishrana u manastiru Studenica: arheozoološka svedočanstva" in *Manastir*
425 *Studenica – arheološka otkrića*, M. Popović, Ed. (Beograd: Republički zavod za zaštitu
426 spomenika kulture i Arheološki institut, 2015), pp. 395–406.
- 427 33. I. Živaljević, N. Marković, M. Maksimović, Food worthy of kings and saints: fish consumption
428 in the medieval monastery Studenica (Serbia). *anth.* **54**, 179–201 (2019).
- 429 34. Marković, N., Radišić, T. & Bikić, "Uloga živine u srednjovekovnoj ekonomiji manastira
430 Studenice" in *Bioarheologija na Balkanu. Metodološke, komparativne i rekonstruktivne studije*
431 *života u prošlosti*, M.-R. N. Vitezović S., Ed. (2016), pp. 99–116.
- 432 35. A. Saed Mucheshi, M. Nikzad, M. Zamani-Dadaneh, Rescue excavations at Bardeh Mar, Darian
433 Dam area, Hawraman, Kurdistan, western Iran. *Proceedings of the 15th* (2017).
- 434 36. M. Mashkour, A. Mohaseb, S. Amiri, S. Beyzaiedoust, R. Khazaeli, H. Davoudi, H. Fathi, S.
435 Komijani, A. Aliyari, H. Laleh, Archaeozoological Report of the Bioarchaeology Laboratory of
436 the University of Tehran and the Osteology Department of the National Museum of Iran, 2015-
437 2016. *Proceedings of the 15th Annual Symposium on the Iranian Archaeology, 5-7 march 2017,*
438 *Tehran, Iranian Center for Archaeological Research*, 803–807 (2017).
- 439 37. P. J. Reimer, W. E. N. Austin, E. Bard, A. Bayliss, P. G. Blackwell, C. B. Ramsey, M. Butzin, H.
440 Cheng, R. Lawrence Edwards, M. Friedrich, P. M. Grootes, T. P. Guilderson, I. Hajdas, T. J.
441 Heaton, A. G. Hogg, K. A. Hughen, B. Kromer, S. W. Manning, R. Muscheler, J. G. Palmer, C.
442 Pearson, J. van der Plicht, R. W. Reimer, D. A. Richards, E. Marian Scott, J. R. Southon, C. S.
443 M. Turney, L. Wacker, F. Adolphi, U. Büntgen, M. Capano, S. M. Fahrni, A. Fogtman-Schulz,
444 R. Friedrich, P. Köhler, S. Kudsk, F. Miyake, J. Olsen, F. Reinig, M. Sakamoto, A. Sookdeo, S.
445 Talamo, The IntCal20 Northern Hemisphere Radiocarbon Age Calibration Curve (0–55 cal
446 kBP). *Radiocarbon.* **62**, 725–757 (2020).
- 447 38. J. Dabney, M. Knapp, I. Glocke, M.-T. Gansauge, A. Weihmann, B. Nickel, C. Valdiosera, N.
448 García, S. Pääbo, J.-L. Arsuaga, M. Meyer, Complete mitochondrial genome sequence of a
449 Middle Pleistocene cave bear reconstructed from ultrashort DNA fragments. *Proc. Natl. Acad.*
450 *Sci. U. S. A.* **110**, 15758–15763 (2013).
- 451 39. M.-T. Gansauge, M. Meyer, Selective enrichment of damaged DNA molecules for ancient
452 genome sequencing. *Genome Res.* **24**, 1543–1549 (2014).
- 453 40. C. Carøe, S. Gopalakrishnan, L. Vinner, S. S. T. Mak, M. H. S. Sinding, J. A. Samaniego, N.
454 Wales, T. Sicheritz-Pontén, M. T. P. Gilbert, Single-tube library preparation for degraded DNA.
455 *Methods Ecol. Evol.* **9**, 410–419 (2018).
- 456 41. H. Jónsson, A. Ginolhac, M. Schubert, P. L. F. Johnson, L. Orlando, mapDamage2.0: fast
457 approximate Bayesian estimates of ancient DNA damage parameters. *Bioinformatics.* **29**, 1682–
458 1684 (2013).
- 459 42. M. Schubert, A. Ginolhac, S. Lindgreen, J. F. Thompson, K. A. S. Al-Rasheid, E. Willerslev, A.
460 Krogh, L. Orlando, Improving ancient DNA read mapping against modern reference genomes.
461 *BMC Genomics.* **13**, 178 (2012).

- 462 43. G. Jun, M. K. Wing, G. R. Abecasis, H. M. Kang, An efficient and scalable analysis framework
463 for variant extraction and refinement from population-scale DNA sequence data. *Genome Res.*
464 **25**, 918–925 (2015).
- 465 44. Broad Institute, *Picard toolkit* (Broad Institute, 2019; <http://broadinstitute.github.io/picard/>).
- 466 45. G. A. Van der Auwera, M. O. Carneiro, C. Hartl, R. Poplin, G. Del Angel, A. Levy-Moonshine,
467 T. Jordan, K. Shakir, D. Roazen, J. Thibault, E. Banks, K. V. Garimella, D. Altshuler, S. Gabriel,
468 M. A. DePristo, From FastQ data to high confidence variant calls: the Genome Analysis Toolkit
469 best practices pipeline. *Curr. Protoc. Bioinformatics.* **43**, 11.10.1–11.10.33 (2013).
- 470 46. B. Langmead, S. L. Salzberg, Fast gapped-read alignment with Bowtie 2. *Nat. Methods.* **9**, 357–
471 359 (2012).
- 472 47. G. Tonkin-Hill, J. A. Lees, S. D. Bentley, S. D. W. Frost, J. Corander, Fast hierarchical Bayesian
473 analysis of population structure. *Nucleic Acids Res.* **47**, 5539–5549 (2019).
- 474 48. J. Corander, P. Marttinen, Bayesian identification of admixture events using multilocus
475 molecular markers. *Mol. Ecol.* **15**, 2833–2843 (2006).
- 476 49. M. A. Suchard, P. Lemey, G. Baele, D. L. Ayres, A. J. Drummond, A. Rambaut, Bayesian
477 phylogenetic and phylodynamic data integration using BEAST 1.10. *Virus Evol.* **4**, vey016
478 (2018).
- 479 50. G. Yu, Using ggtree to Visualize Data on Tree-Like Structures. *Curr. Protoc. Bioinformatics.* **69**,
480 e96 (2020).
- 481 51. M. Krzywinski, J. Schein, Í. Birol, J. Connors, R. Gascoyne, D. Horsman, S. J. Jones, M. A.
482 Marra, Circos: An information aesthetic for comparative genomics. *Genome Res.* **19**, 1639–1645
483 (2009).
- 484 52. A. Stamatakis, RAxML version 8: a tool for phylogenetic analysis and post-analysis of large
485 phylogenies. *Bioinformatics.* **30**, 1312–1313 (2014).
- 486 53. A. J. Page, B. Taylor, A. J. Delaney, J. Soares, T. Seemann, J. A. Keane, S. R. Harris, SNP-sites:
487 rapid efficient extraction of SNPs from multi-FASTA alignments. *Microb Genom.* **2**, e000056
488 (2016).
- 489 54. P. O. Lewis, A likelihood approach to estimating phylogeny from discrete morphological
490 character data. *Syst. Biol.* **50**, 913–925 (2001).
- 491 55. K. Katoh, D. M. Standley, MAFFT multiple sequence alignment software version 7:
492 improvements in performance and usability. *Mol. Biol. Evol.* **30**, 772–780 (2013).
- 493 56. P. J. A. Cock, T. Antao, J. T. Chang, B. A. Chapman, C. J. Cox, A. Dalke, I. Friedberg, T.
494 Hamelryck, F. Kauff, B. Wilczynski, M. J. L. de Hoon, Biopython: freely available Python tools
495 for computational molecular biology and bioinformatics. *Bioinformatics.* **25**, 1422–1423 (2009).
- 496 57. W. Shen, S. Le, Y. Li, F. Hu, SeqKit: A Cross-Platform and Ultrafast Toolkit for FASTA/Q File
497 Manipulation. *PLoS One.* **11**, e0163962 (2016).
- 498 58. H. Li, seqtk Toolkit for processing sequences in FASTA/Q formats. *GitHub.* **767**, 69 (2012).
- 499 59. S. Duchêne, D. Duchêne, E. C. Holmes, S. Y. W. Ho, The Performance of the Date-
500 Randomization Test in Phylogenetic Analyses of Time-Structured Virus Data. *Mol. Biol. Evol.*
501 **32**, 1895–1906 (2015).

- 502 60. A. Rieux, F. Balloux, Inferences from tip-calibrated phylogenies: a review and a practical guide.
503 *Mol. Ecol.* **25**, 1911–1924 (2016).
- 504 61. M. Navascués, F. Depaulis, B. C. Emerson, Combining contemporary and ancient DNA in
505 population genetic and phylogeographical studies. *Mol. Ecol. Resour.* **10**, 760–772 (2010).
- 506 62. S. Duchene, P. Lemey, T. Stadler, S. Y. W. Ho, D. A. Duchene, V. Dhanasekaran, G. Baele,
507 Bayesian Evaluation of Temporal Signal in Measurably Evolving Populations. *Mol. Biol. Evol.*
508 **37**, 3363–3379 (2020).
- 509 63. G. Baele, P. Lemey, M. A. Suchard, Genealogical Working Distributions for Bayesian Model
510 Testing with Phylogenetic Uncertainty. *Syst. Biol.* **65**, 250–264 (2016).
- 511 64. M. Molak, M. A. Suchard, S. Y. W. Ho, D. W. Beilman, B. Shapiro, Empirical calibrated
512 radiocarbon sampler: a tool for incorporating radiocarbon-date and calibration error into
513 Bayesian phylogenetic analyses of ancient DNA. *Mol. Ecol. Resour.* **15**, 81–86 (2015).
- 514 65. F. Rodríguez, J. L. Oliver, A. Marín, J. R. Medina, The general stochastic model of nucleotide
515 substitution. *J. Theor. Biol.* **142**, 485–501 (1990).
- 516 66. Z. Yang, Maximum likelihood phylogenetic estimation from DNA sequences with variable rates
517 over sites: approximate methods. *J. Mol. Evol.* **39**, 306–314 (1994).
- 518 67. A. J. Drummond, S. Y. W. Ho, M. J. Phillips, A. Rambaut, Relaxed phylogenetics and dating
519 with confidence. *PLoS Biol.* **4**, e88 (2006).
- 520 68. B. Pfeifer, U. Wittelsbürger, S. E. Ramos-Onsins, M. J. Lercher, PopGenome: an efficient Swiss
521 army knife for population genomic analyses in R. *Mol. Biol. Evol.* **31**, 1929–1936 (2014).
- 522 69. D. K. Ajithdoss, S. M. Reddy, P. F. Suchodolski, L. F. Lee, H.-J. Kung, B. Lupiani, In vitro
523 characterization of the Meq proteins of Marek’s disease virus vaccine strain CVI988. *Virus Res.*
524 **142**, 57–67 (2009).
- 525 70. T. Huszár, I. Mucsi, T. Terebessy, A. Masszi, S. Adamkó, C. Jeney, L. Rosivall, The use of a
526 second reporter plasmid as an internal standard to normalize luciferase activity in transient
527 transfection experiments may lead to a systematic error. *J. Biotechnol.* **88**, 251–258 (2001).
- 528 71. K.-S. Chang, K. Ohashi, M. Onuma, Diversity (polymorphism) of the meq gene in the attenuated
529 Marek’s disease virus (MDV) serotype 1 and MDV-transformed cell lines. *J. Vet. Med. Sci.* **64**,
530 1097–1101 (2002).
- 531 72. I. Letunic, P. Bork, Interactive tree of life (iTOL) v3: an online tool for the display and
532 annotation of phylogenetic and other trees. *Nucleic Acids Res.* **44**, W242–5 (2016).
- 533 73. J. Sato, S. Murata, Z. Yang, B. B. Kaufer, S. Fujisawa, H. Seo, N. Maekawa, T. Okagawa, S.
534 Konnai, N. Osterrieder, M. S. Parcells, K. Ohashi, Effect of Insertion and Deletion in the Meq
535 Protein Encoded by Highly Oncogenic Marek’s Disease Virus on Transactivation Activity and
536 Virulence. *Viruses.* **14** (2022), doi:10.3390/v14020382.
- 537 74. C. Firth, A. Kitchen, B. Shapiro, M. A. Suchard, E. C. Holmes, A. Rambaut, Using time-
538 structured data to estimate evolutionary rates of double-stranded DNA viruses. *Mol. Biol. Evol.*
539 **27**, 2038–2051 (2010).

540 **Acknowledgments:**

541 This research used the University of Oxford’s Advanced Research Computing, Queen Mary’s
542 Apocrita, and the Leibniz-Rechenzentrum (LRZ) High Performance Computing facility.

543
544
545
546
547
548
549
550
551
552
553
554
555
556
557
558
559
560
561
562
563
564
565
566
567
568
569
570
571

Funding:

European Research Council grant ERC-2019-StG-853272-PALAEOFARM or ERC-2013-StG-337574-UNDEAD or both (SRF, LAF, GL, ALS)
Wellcome Trust grant 210119/Z/18/Z (SRF, LAF)
Oxford Martin School grant ATR02370 (SRF, ALS, LdP, OGP)
AHRC grant AH/L006979/1 (GL, OL, NS)
European Union’s Horizon 2020 research and innovation programme under the Marie Skłodowska-Curie grant agreement no. 895107 (OL)
BBSRC grant number BB/M011224/1 (SD)
Postdoctoral grant (12U7121N) of the Research Foundation -- Flanders (Fonds voor Wetenschappelijk Onderzoek) (BV)

Author contributions:

Conceptualization: SRF, ALS, LAFF, GL
Methodology: SRF, EAD, ALS, LAFF, GL, BV, LdP, VN, OL, OGP
Sample provision: OL, NM, GF, RS, HB, LDS, DNS, IVA, OP, MS, HD, HF, ASM, AAV, AF, NS, JB, AOA, OVA, MM, VN
Investigation: SRF, EAD, OL, LdP, BV, SC, AFH, KT, PGF, SD, HL, GCB, OGP, VN, GL, ALS, LAFF
Visualization: SRF
Funding acquisition: LAFF, ALS, GL
Project administration: SRF, LAFF, ALS, GL
Supervision: LAFF, ALS, GL
Writing – original draft: SRF, LAFF, ALS, GL
Writing – review & editing: SRF, EAD, OL, LdP, BV, SC, AFH, KT, PGF, SD, NM, HL, GF, RS, HB, LDS, DNS, IVA, OP, MS, HD, HF, ASM, AAV, AF, NS, GCB, JB, AOA, OVA, MM, OGP, VN, GL, ALS, LAFF

Competing interests:

The authors declare that they have no competing interests.

Data and materials availability:

All MDV sequence data generated have been deposited in GenBank under accession PRJEB64489. Code is available at GitHub (<https://github.com/antonisdim/MDV>) and archived at Zenodo (<https://zenodo.org/records/10022436>) (25).

Supplementary Materials:

Materials and Methods
Supplementary Text

583 Figs. S1 to S9
584 Tables S4, S9 and S10
585 Captions for Data S1
586 References (26-74)

587

588 **Other Supplementary Materials for this manuscript include the following:**

589

590 Data S1, which comprises:

591

- Table S1: Sample metadata

592

- Table S2: Screening and capture sequencing results

593

- Table S3: Modern genome metadata

594

- Table S5: Integrity of miRNA sequences in ancient MDV

595

- Table S6: Fixed differences between ancient and modern MDV strains

596

- Table S7: PAML results

597

- Table S8: *Meq* sequence metadata

598

- Table S11: Metagenomic screening summary data

599

- Table S12: SNP summary table

600

- Table S13: Tip dates for BEAST analysis